A Time-dependent Quantum Dynamics Study of the $H_2 + CH_3 \rightarrow H + CH_4$ Reaction

Dunyou Wang[a]

Eloret, NASA Ames Research Center, Mail Stop T27B-1, Moffett Feild, CA 94035-1000

ABSTRACT

We present a time-dependent wave-packet propogation calculation for the $H_2 + CH_3 \rightarrow H + CH_4$ reaction in six degrees of freedom and for zero total angular momentum. Initial state selected reaction probability for different initial rotational-vibrational states are presented in this study. The cumulative reaction probability (CRP) is obtained by summing over initial-state-selected reaction probability. The energy-shift approximation to account for the contribution of degrees of freedom missing in the 6D calculation is employed to obtain an approximate full-dimensional CRP. Thermal rate constant is compared with different experiment results.

[a] Electronic mail: dywang@nas.nasa.gov

I. INTRODUCTION

The reaction $H + CH_4 \rightarrow H_2 + CH_3$ and its reverse reaction $CH_3 + H_2 \rightarrow H + CH_4$ are of obvious importance in methane pyrolysis and combustion [1]. In addtion, the reverse reaction also plays an important role in the modeling of the chemistry of hydrocarbons in the atmospheres of giant planets [2]. Numerous experimental [3–12] and theoretical studies [13–18] have been reported on these two reactions. Recently, the forward reaction $H + CH_4 \rightarrow H_2 + CH_3$ has become the focus of a number of quantum dynamics calculations [19–26] in reduced dimensionality and a full-dimensional transit state flux method quantum calculation. Nevertheless, no quantum dynamics studies have been reported on the reverse reaction $H_2 + CH_3 \rightarrow H + CH_4$ so far.

In the reduced dimensional [19,20,23,24] calculations for the forward reaction $H + CH_4 \rightarrow H_2 + CH_3$, usually energy shifting [27–29] methods are needed to obtain approximate full dimentionality cumulative reaction probability for zero angular momentum J, and J-K shifting methods [27–29] are employed to calculate total cumulative reation probability for the full dimensionality rate constants for both reduced dimensional and full dimensional calculations [22,25]. In the reduced dimensional quantum calculations, initial stated selected reaction probabilities were calculated. However, for the full dimensional calculation, the calculations were limited to the CRP only due to the limition of the transit state flux method calculation to obtain initial state selected reaction probability, as well as due to the difficulty of calculations in full dimensionality.

All the quantum calculations mentioned above were done using the twelve degrees of freedom potentional energy surface of Jordan and Gilbert [30]. This potential has a $C_{3\nu}$ transition state with a collinear structure of $H - H - C$ and the center of mass of H_3. The vibrationally adiabatic barrier height of this potential energy surface is 10.9 kcal/mol for the forward reaction, $H + CH_4 \rightarrow H_2 + CH_3$ and 11.0 kcal/mod for the reverse reaction, $H_2 + CH_3 \rightarrow H + CH_4$, respectively. This potential energy surface is based in part on previous *ab initio* calculations of the saddle point, as well as on a previous, semiglobal

potential used in variational transition state theory calculations fo the rate constant. The rate constant from the theoretical calculations of the forward reaction, comparing to the experiment, indicates that the barrier height on the Jordan-Gilbert potential may be too low.

In this paper, we report six degrees of freedom, time -dependent quantum calculations of the reaction $H_2 + CH_3 \rightarrow H + CH_4$, by treating the reaction as a diatom-diatom reaction system and carry out a full dimensional quantum dynamics calculation for this pseudo diatom-diatom reaction. Initial state selected reaction probability, cumulative reaction probability(CRP), and thermal rate constant are calculated. We apply energy shifting method to obtain the thermal rate constants and compare our results with experiments.

This paper is organized as follows: Section II briefly reviews the theory used in this calculation and the energy-shifting methods are also presented. Section III gives numerical results of the calculation, and section IV concludes.

II. THEORY AND METHODS

A. Time-dependent wave-packet propogation method

This study employs the time-dependent wave-packet propogation method [31–33] to carry out the quantum dynamics calculation. The reverse reaction, $H_2 + CH_3 \rightarrow H + CH_4$, is treated as a diatom-diatom reaction, $H_2 + CX \rightarrow H + HCX$, where X is a pseudoatom with the mass of the three unreactive hydrogen atoms and located at their center of mass. The vibrational motion of CX approximately represents the umbrella motion of CH_3, where the three hydrogen atoms move in phase , and the $C - H$ bond length is fixed at its equalibrium geometries. Thus the reduced dimensionality calculation for this pseudo diatom-diatom is six degrees of freedom.

The Hamiltonian for this model system in the reactant Jacobi coordinates is given by

$$H = -\frac{\hbar^2}{2\mu}\frac{\partial^2}{\partial R^2} + \frac{(J-j)^2}{2\mu R^2} + h_{r_1}(r_1) + h_{r_2}(r_2) + \frac{j_1^2}{2\mu_1 r_1^2} + \frac{j_2^2}{2\mu_2 r_2^2} + V(R, r_1, r_2, \theta_1, \theta_2, \phi), \quad (1)$$

where μ is the reduced mass of H_2 with respect to the center of mass of the pseudo diatom CX, r_1 is the distance for H_2, r_2 is the distance between C and X, R is the distance from the center of mass of H_2 to the center of mass of CX, **J** is the total angular momentum operator, $\mathbf{j_1}$ and $\mathbf{j_2}$ are the rotational angular momentum operators for H_2 and pseudo diatom CX respectively, θ_1 and θ_2 are the two Jacobi angles between R and r_1 and R and r_2, ϕ is the torsion angle. The diatomic reference Hamiltonians $h_{r_1}(r_1)$ and $h_{r_2}(r_2)$ are defined as

$$h_{r_1}(r_1) = -\frac{\hbar^2}{2\mu_1}\frac{\partial^2}{\partial r_1^2} + V(r_1),$$
$$h_{r_2}(r_2) = -\frac{\hbar^2}{2\mu_2}\frac{\partial^2}{\partial r_2^2} + V(r_2). \tag{2}$$

Where $V(r_1)$ and $V(r_2)$ are the one-dimensional reference potentials for H_2 and CX and the μ_1 and μ_2 are the corresponding reduced masses. The 1D potentials are the potential cuts in the respective coordinates with the system in the reactant chanel and all other coordinates are fixed at their equilibium geometry.

The time-dependent wave function can be expanded in terms of the body-fixed (BF) rovibrational eigenfunctions defined in terms of the reactant Jacobi coordinates as

$$\Psi^{JM\epsilon}_{\nu jK} = \sum_{n\nu_1\nu_2 j_1 j_2 K} F^{JM\epsilon}_{n\nu_1\nu_2 j_1 j_2 K,\nu jK}(t)\mu^{\nu_2}_n(R)\phi_{\nu_1}(r_1)\phi_{\nu_2}(r_2)Y^{JM\epsilon}_{jK}(\theta_1,\theta_2,\phi), \tag{3}$$

where n in the translational basis label, and sine DVR basis are used as the translational basis, ϵ is the parity of the system. ϕ_{ν_1} and ϕ_{ν_2} are the eigenfunctions of the reference Hamiltonia in Eq.(2). The angular momentum basis function $Y^{JM\epsilon}_{jK}(\theta_1,\theta_2,\phi)$ is the BF, parity adapted, total angular momentum eigenfunction, which can be written as

$$Y^{JM\epsilon}_{jK} = \frac{1}{\sqrt{2(1+\delta_{K0})}}[Y^{JM}_{j_1 j_2 j_{12}K} + \epsilon(-1)^{(j_1+j_2+j_{12}+J)}Y^{JM}_{j_1 j_2 j_{12}-K}] \tag{4}$$

where

$$Y^{JM}_{j_1 j_2 j_{12}K} = D^J_{MK}(\alpha,\beta,\gamma)Y^{j_{12}K}_{j_1 j_2} \tag{5}$$

$D^J_{MK}(\alpha,\beta,\gamma)$ is the normalized Wigner rotation maxtrix and $Y^{j_{12}K}_{j_1 j_2}$ is the angular momentum eigenfunction of j_{12}

$$Y_{j_1 j_2}^{j_{12} K} = \sum_{m_1} < j_1 m_1 j_2 K - m_1 | j_{12} K > y_{j_1 m_1}(\theta_1, 0) y_{j_2 K - m_1}(\theta_2, \phi), \tag{6}$$

with y_{jm} the spherical harmonics.

The split-operator method is employed to propogate the wave packet

$$\psi^{JM\epsilon}(\mathbf{R}, \mathbf{r_1}, \mathbf{r_2}, t + \Delta) = e^{-iH_0\Delta/2} e^{-iU\Delta} e^{-iH_0\Delta/2} \psi^{JM\epsilon}(\mathbf{R}, \mathbf{r_1}, \mathbf{r_2}, t). \tag{7}$$

The reference Hamiltonian H_0 is defined as

$$H_0 = -\frac{\hbar^2}{2\mu}\frac{\partial^2}{\partial R^2} + h_{r_1}(r_1) + h_{r_2}(r_2), \tag{8}$$

and the effictive potential operator in Eq. (7)

$$U = \frac{(J-j)^2}{2\mu R^2} + \frac{j_1^2}{2\mu_1 r_1^2} + \frac{j_2^2}{2\mu_2 r_2^2} + V(R, r_1, r_2, \theta_1, \theta_2, \phi). \tag{9}$$

The initial wave-packet is chosen as the product of specific initial rovibrational states of the diatom H_2 and pesudo diatom CX and a localized standard Gaussian function $\Phi_{k_0}(R)$

$$\Psi_{n_0 \nu_0 j_0 K_0}(t = 0) = \Phi_{k_0}(R) \phi_{\nu_{10} j_{10}}(r_1) \phi_{\nu_{20} j_{20}}(r_2) Y_{j_{10} j_{20} j_{120} K_0}^{JM\epsilon}. \tag{10}$$

Fianlly, the initial-state-selected reaction probability is extracted from the time-dependent reactive flux in the standard way.

B. Cumulative reaction probability and thermal rate constant

In order to obtain an approximate full dimensional(12D) cumulative reaction probability(CRP) for J=0 and thermal rate constant, we first calculate the reduced dimensional(6D) CRP(J=0), denoted $N^{J=0,rd}(E)$, by summing over all the initial state-selected rovibrational reaction probability $P_{\nu_1 \nu_2 j_1 j_2}^{J=0}(E)$,

$$N^{J=0,rd}(E) = \sum_{\nu_1, \nu_2 = 0} \sum_{j_1, j_2 = 0}, P_{\nu_1 \nu_2 j_1 j_2}^{J=0}(E) \tag{11}$$

where E is the total Energy.

Our reduced dynamics calculation has six degrees of freedom, while the H_2+CH_3 reaction system has twelve degrees of freedom. So the energy shifting method has to be applied to obtain the CRP for the full dimensionality using our reduced dimensional calculation. Thus

$$N^{J=0,full} = \sum_{\nu_1\nu_2,...,\nu_6} N^{J=0,rd}(E - E^{\ddagger}_{\nu_1\nu_2,...,\nu_6}). \tag{12}$$

here $\nu_1\nu_2, ..., \nu_6$ are the quantum numbers of the six vibrational degrees of freedom of the transition state, which are not included in our reduced dimensional calculation. These energies are given in the harmonic approximation by

$$E^{\ddagger}_{\nu_1\nu_2,...,\nu_6} = \sum_{i=1}^{6} \hbar\omega_i^{\ddagger}(\nu_i + \frac{1}{2}). \tag{13}$$

The J-K shifting method is employed here to calculate the CRP for nonzero total angular momentum J. The total CRP, $N(E)$ is defined as the sum of CPRs of all the open J and K channels

$$N(E) = \sum_{J=0}(2J+1) \sum_{K=-J}^{J} N^{J=0,full}(E - E^{\ddagger}_{JK}), \tag{14}$$

where $E^{\ddagger}_{JK}$ is the rigid rotor rotational energy of the reaction system at the transition state. In the present case, the system at transition state is a well defined symmetric top

$$E^{\ddagger}_{JK} = B^{\ddagger}J(J+1) + (A^{\ddagger} - B^{\ddagger})K^2. \tag{15}$$

$A^{\ddagger}$ and $B^{\ddagger}$ are the rotational constants of H_2CH_3 at the full dimensional transition state.

The thermal rate constant can be computed exactly from the expression

$$k(T) = \frac{1}{hQ_{react}} \int_0^{\infty} N(E)e^{-E/k_BT}dE. \tag{16}$$

The above equation simplifies in the J-K shifting approximation, Eq. (14), to

$$k(T) = \frac{Q^{\ddagger}_{rot}}{hQ_{react}} \int_0^{\infty} N(E)e^{-E/k_BT}dE, \tag{17}$$

where $Q^{\ddagger}_{rot}$ is the rotational partition function of the reaction system at the transition state and Q_{react} is the reactant partition function, which is written as a product of vibrational,

rotational, and translational partition functions. As noted in Ref. [24], the consistent approach to calculate the vibrational partition function of CH_3 is to combine the results of the reduced dimensional quantum calculations with the 'missing' vibrational frequencies which are not included in the reduced dimensonality. The purpose of doing this is to be consistent with the procedure that we use to convert the full dimensional CRP from the reduced dimensional CRP in Eq. (12).

III. RESULTS AND DISCUSSION

A. Numerical aspects

The numerical parameters used in this work are: 60 sine basis functions for the translational grid of R in the range of [2.7, 10.0] Bohr, 30 H_2 optimized vibrational basis functions for the r_1 coordinates, 4 optimized CX vibrational basis functions ofr the r_2 coordinates, and total 1092 coupled angular momentum basis used for the angular part. The wave-packet was propogated with a time step of 15 for a total time of 6000 a.u. The rotational constants, $A^{\ddagger}$ and $B^{\ddagger}$ in Eq. (15), are 5.12 cm^{-1} and 2.00 cm^{-1}. The vibrational frequencies [24] that are 'missing' in our reduced dimensional calculations at the transition state are: 589 $cm^{-1}(2)$, 1439 $cm^{-1}(2)$, 2959cm^{-1} and 3092$cm^{-1}(2)$. These 'missing' vibrational frequencies are used to obtain the full dimensionality CRP for J=0 in Eq.(12).

B. Initial-state-selected probability

Fig. 1 shows the reaction probability for the first four initial vibrational states of $H_2(\nu_1, j_1{=}0)$ with CX at ground state($\nu_2{=}j_2{=}0$) as a function of kinetic energy. As seen, vibrational excitation of H_2 enhances this reactivity by lowing the reaction threshold. Fig. 1 also shows resonance-like structures in these vibrational excitation probability. And this feature has also been seen in the forward reaction, $H + CH_4$ [21,24], which indicates that the dynamical resonances exist in these reactions. The reaction probabitily of vibrational exciation of

$CX(\nu_2, j_2{=}0, \nu_1{=}j_2{=}0)$ are plotted in Fig. 2. Comparing to Fig.1, The reaction probability decreases as the vibrational excitation of CX increases. This is understandable due to that CX mainly funtions as a spector in this reaction. The more of the CH_3 vibrates, the harder for H atom in H_2 to 'catch' the C atom in CH_3.

The rotational excitation probability of H_2, with $\nu_1{=}1$, $\nu_2{=}j_2{=}0$, for j_1 up to 5 is given in Fig. 3 as a function of kinetic energy. In Fig. 3, $j_1{=}0$ rotational state of H_2 gives the largest reaction probability. Comparing to Fig. 4, which is the reaction probability for different CX rotational states , $j_2{=}1$ initial rotational state has the largest reaction probability. This is because H_2 is much more vibrationally active than CX, and as a result, the isotropic rotational function of $H_2(\nu_1{=}1,\ j_1{=}0)$ has a larger radius, which ensures a bigger overlap between the rotational wavefuction of $H_2(j_1{=}0)$ and $CX(\nu_2{=}j_2{=}0)$ than that of $H_2(j_1{=}1)$, whose rotational wavefunction only distributes along the r_1 coordinate. So the reaction is more favorable to $H_2(j_1{=}0)$ initial state in Fig. 3. On the contrary, the initial $CX(j_2{=}0)$ state has a smaller radius of the isotropic rotational wavefuction, while the $CX(\nu_2{=}1,\ j_2{=}1)$ initial state, which distributes along the r_2 bond, has the bigger overlap with $H_2(\nu_1{=}j_1{=}0)$ at the linear transition state with C atom facing either H atom in H_2. This explains why the $CX(j_2{=}1)$ initial state has the larger reaction probability in Fig. 4. Also one can see that the rotational excitations of H_2 have the bigger effect on the reaction probability than those of CH_3.

C. Cumulative reaction probability and thermal rate constant

A normal mode analysis is performed to determine the 'missing' modes in our reduced dimensional quantum calculation, as also seen in Ref. [24]. Then Eq.(12) is used to obtain the full dimensional CRP for J=0. For total scattering energy up to 2.1 eV, all the missing modes given in Section A. contribute to convert the full dimensional CRP from the six degrees of freedom quantum calculation. And the full dimensional converted CPR is shown in Fig. 5 as a function of the total energy, which includes the difference between our six

degrees of freedom ZPE and the full dimensional normal mode ZPE, 0.936 eV. Using the harmonic approximation of the 'missing' degrees of freedom in CH_3 is consistent with using this approximation in the energy shifting expression in Eq. (12).

The resulting rate constant, obtained using $J-K$ shifting is shown in Fig. 6 along with several different experiments. This figure shows that the present six dof calculation is larger than the experiments, espcially in the low temperature range. This feature, theoretical rate constant larger than the experiment, is also shown in the foward reaction $H + CH_4$ [19,20,22–25]. Thus present study of the reverse reaction of $H_2 + CH_3$ supports the earlier studies on $H + CH_4$ and that barrier on the Jordan-Gilbert potential is too low.

IV. SUMMARY AND CONCLUSIONS

A six degree-of-freedom, time-dependent wavepacket propogation method, has been performed for the reaction, $H_2 + CH_3 \rightarrow H + CH_4$, by treating the reaction system as a pesudo-diatom-diatom reaction system. The energy-shifting method has been employed to obtain the full dimensional cumulative reaction probability for J=0. And $J-K$ shifting approach is applied to this CRP to obtain the thermal rate constant which is compared with different experiments. A potential surface due to Jordan and Gilbert, which has been used in previous quantum calculation of the forward reaction $H + CH_4 \rightarrow H_2 + CH_3$, was used in these calculations.

Initial state selected reaction probability and the cumulative reaction probability were calculated for zero total angular momentum. The vibrational excitations of H_2 bond substantially enhance the reaction probability. The vibrational excitations of CH_3 cause difficulity for H in H_2 to 'capture' C atom, thus it has smaller effect on the reaction probability. The $j_2 = 1$ initial states of CH_3 gives the largest reaction probability comparing to $j_1 = 0$ of H_2, this feature needs to be further investigated in furture work.

Energy shifting method was used to convert the reduced dimensional CRP for zero total angular momentum to a full dimensional one. And our rate constant is larger than the

experiment, an indication that the barrier on the Jordan-Gilbert potential is most likely too low.

V. ACKNOWLEDGEMENTS

This work is supported by NASA prime contract NAS2-00062. D.Y.W. thanks Dr. Winifred Huo and Dr. David Schwenke for stimulating discussions on the subject.

REFERENCES

[1] J. Warnatz, in *Combustion Chemistry*, edited by W.C. Jr. (Springer-Verlag, New York, 1984).

[2] A. Fahr, P.S. Monks, L.J. Stief and A.H. Laufer, Icarus **116**,, 415 (1995).

[3] C.P. Fenimore and G.W. Jones J. Phys. Chem. **65**, 200 (1961).

[4] J. Peeters, G. Mahnen, *14th Symposium (international) on Combustion*, (The Combustion Institute, Pittsburgh, 1973).

[5] J.C. Biordi, C.P. Lazzara and J.F. Papp, Combust. Flame **26**, 57 (1976).

[6] P. Roth and T. Just, Ber. Bunsenges. Phys. Chem. **79**, 682 (1975).

[7] R. Shaw, J. Phys. Chem. Ref. Data **7**, 1179 (1978).

[8] W. Moller and E. Mozzhukhin and H.G. Wagner, Ber. Bunsenges. Phys. Chem. **90**, 854 (1980).

[9] M.J. Rabinowitz, J.W. Sutherland, P.M. Patterson and R.B. Klemm, J. Phys. Chem. **95**, 674 (1991).

[10] H.J. Baeck, K.S. Shin, H. Yang, Z. Qing, V. Lissianski and W.C Gardiner, Jr., J. Phys. Chem. **99**, 15925 (1995).

[11] V.D. Knyazev, A. Bencsura, S.I. Stoliarov and I.R. Slagle J. Phys. Chem. **100**, 11346 (1996).

[12] J.W. Sutherland M.C. Su and J.V. Micheal, Inter. J. Chem. Kinet. **33**, 69 (2001).

[13] T.C. Clark, J.E. Dove, J. Chem. Phys. **51**, 2147 (1973).

[14] L.M. Raff J. Chem. Phys. **60**, 2220 (1974).

[15] G.C. Schatz, A.F. Wagner and T.H. Dunning J. Phys. Chem. **88**, 221 (1984).

[16] R. Steckler, K.J. Dykema, K.J. Brown, F.B. Hancock and D.G. Truhlar J. Chem. Phys. **87**, 7024 (1987).

[17] T. Joseph, R. Steckler and D.G. Truhlar J. Chem. Phys. **87**, 1036 (1987).

[18] J. Pu and D.G. Truhlar, J. Chem. Phys. **116**, 1468 (2002).

[19] T. Takayanagi, J. Chem. Phys. **104**, 2237 (1996).

[20] H.-G. Yu and G. Nyman, J. Chem. Phys. **111**, 3508 (1999).

[21] M.L. Wang, Y. Li , J.Z.H. Zhang and D.H. Zhang, J. Chem. Phys. **113**, 1802 (2000).

[22] F. Huarte-Larrañaga and U. Manthe J. Chem. Phys. **113**, 5115 (2000)

[23] J.M. Bowman, D.Y. Wang, X.C. Huang, F. Huarte-Larrañaga and U. Manthe J. Chem. Phys. **114**, 9683 (2001).

[24] D.Y. Wang and J.M. Bowman J. Chem. Phys. **115**, 2055 (2001).

[25] F. Huarte-Larrañaga and U. Manthe J. Chem. Phys. **116**, 2863 (2002)

[26] M.L. Wang and J.Z.H. Zhang J. Chem. Phys. **116**, 6497 (2002).

[27] J.M. Bowman J. Phys. Chem. **95**, 4950 (1991).

[28] J.M. Bowman, in *Reaction and Molecular Dynamics Proceedings of the European School on Computational Chemistry, Perugia, Italy,* July(1999), edited by A. Lagana and A. Riganelli (Springer, New York, 2000).

[29] J.M. Bowman and A. F. Wagner, in *The Theory of Chemical Reaction Dynamics*, edited by D.C. Clary (Reidel, Dordrecht, 1986).

[30] M. Jordan and R. Gilbert, J. Chem. Phys. **102**, 5669 (1995).

[31] D.H. Zhang and J.Z.H. Zhang, J. Chem. Phys. **100**, 2687 (1993).

[32] D.H. Zhang and J.Z.H. Zhang, J. Chem. Phys. **101**, 1446 (1994).

[33] Y.C. Zhang, D. Zhang, W. Li, Q.G. Zhang, D.Y. Wang D.H. Zhang and J.Z.H. Zhang J. Phys. Chem. **99**, 16824 (1995).

Fig. 1 The initial state selected reaction probability for the reaction $H_2(\nu_1, j_1 = 0) + CH3(\nu_2 = j_2 = 0) \rightarrow H + CH_4$ as a function of kinetic energy (J=0).

Fig. 2 Same as Fig. 1 but for the vibrational excitations of $CH_3(\nu_2, j2 = 0)$ with $H_2(\nu_1 = j_1 = 0)$.

Fig. 3 The initial state selected reaction probability for the reaction $H_2(\nu_1 = 0, j_1) + CH3(\nu_2, j_2 = 0) \rightarrow H + CH_4$ as a function of kinetic energy (J=0).

Fig. 4 Same as Fig. 3 but for the rotational excitations of $CH_3(\nu_2 = 0, j2)$

Fig. 5 The cumulative reaction probability $N^{J=0,full}(E)$ as a function of total energy.

Fig. 6 Comparison of the present reduced dimensionality thermal rate constant with different experiments. [1] Ref. [12] , [2] Ref. [9] , [3] Ref. [7] , [4] Ref. [11].

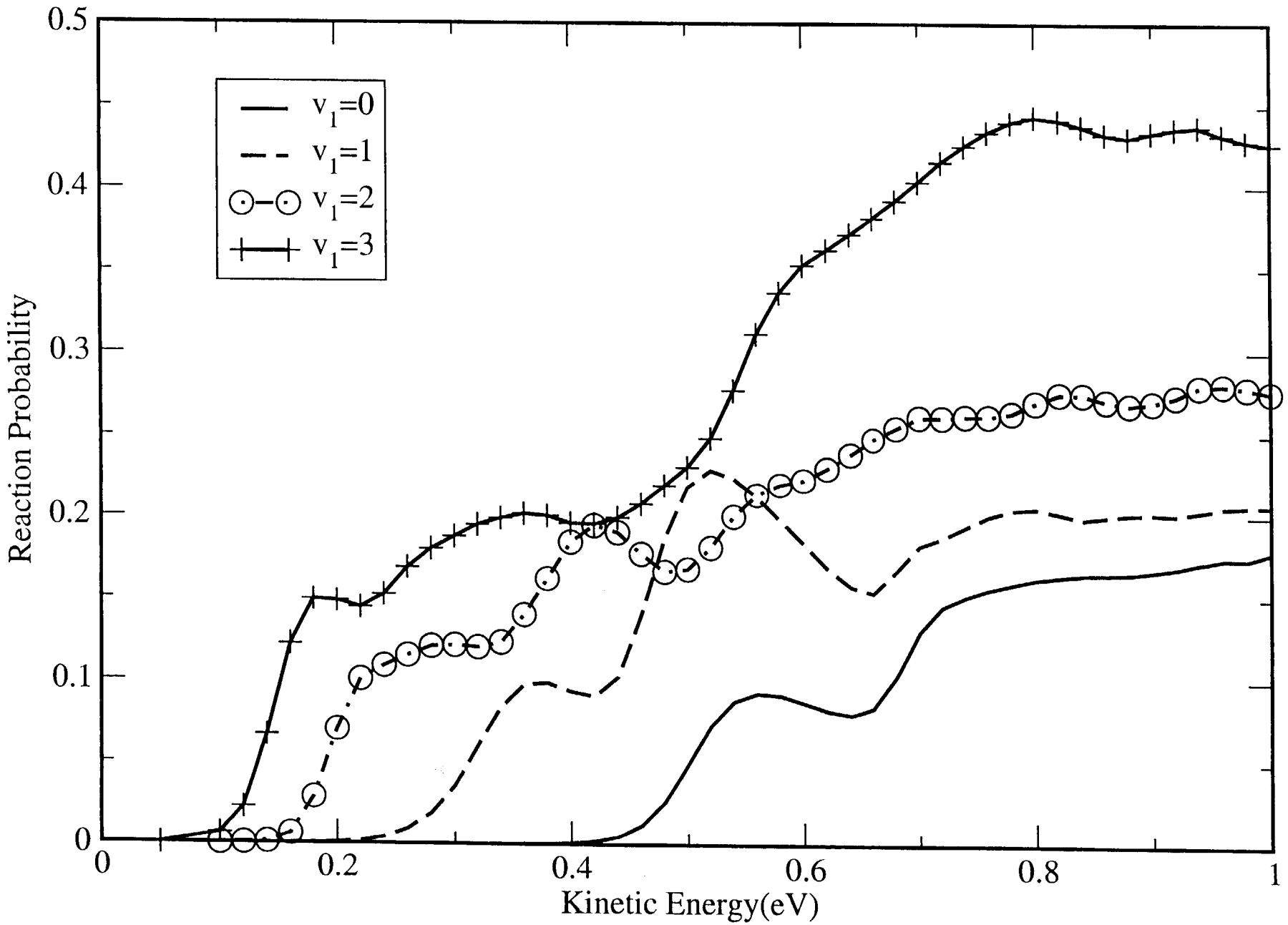
0.5
0.4
0.3
0.2
0.1
0
0
0.2
0.4
0.6
0.8
1
Reaction Probability
Kinetic Energy(eV)
v1=0
v1=1
v1=2
v1=3

Fig. 1

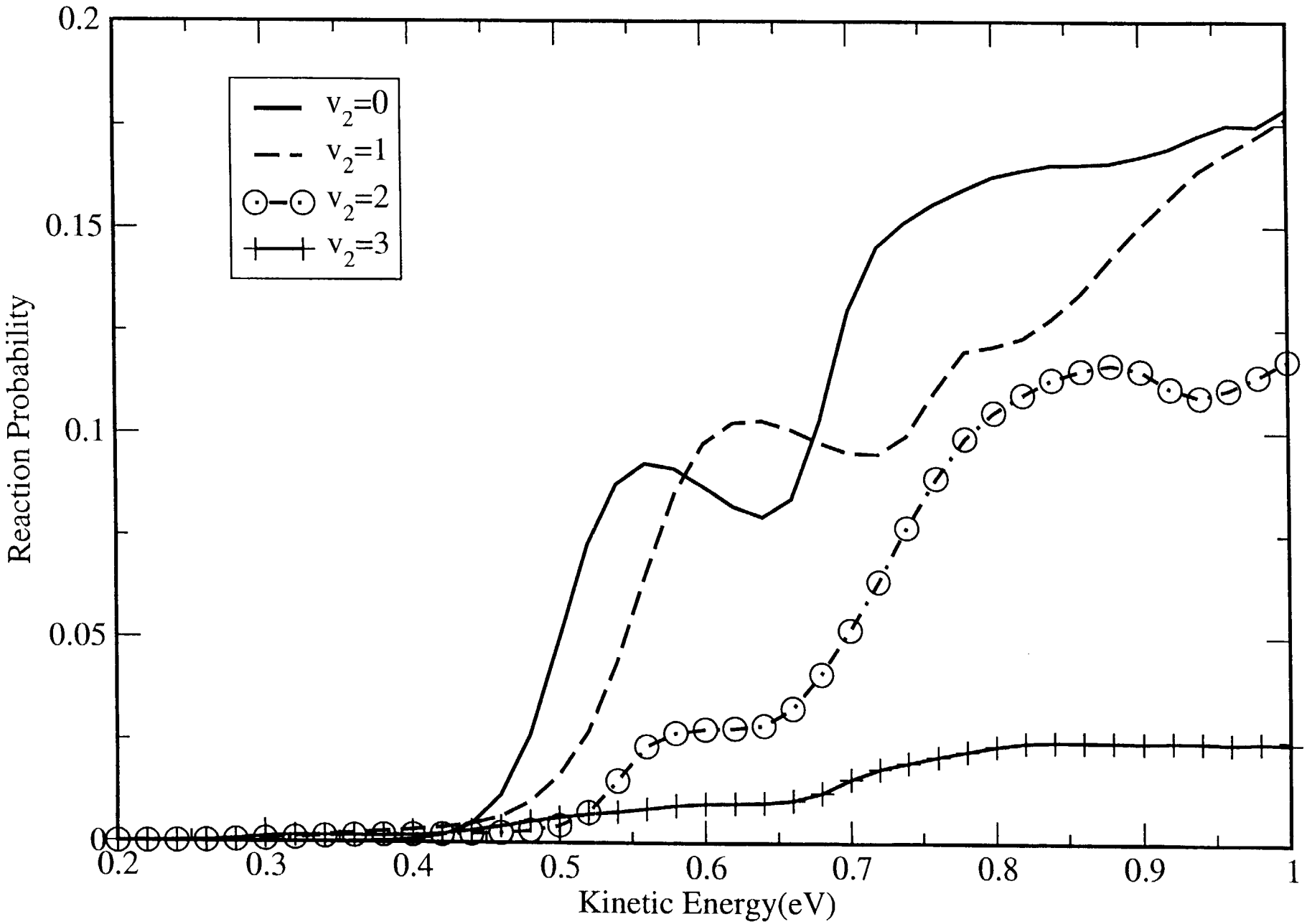
0.2
0.15
0.1
0.05
0
Reaction Probability
v_2=0
v_2=1
v_2=2
v_2=3
0.2
0.3
0.4
0.5
0.6
0.7
0.8
0.9
1
Kinetic Energy(eV)

Fig. 2

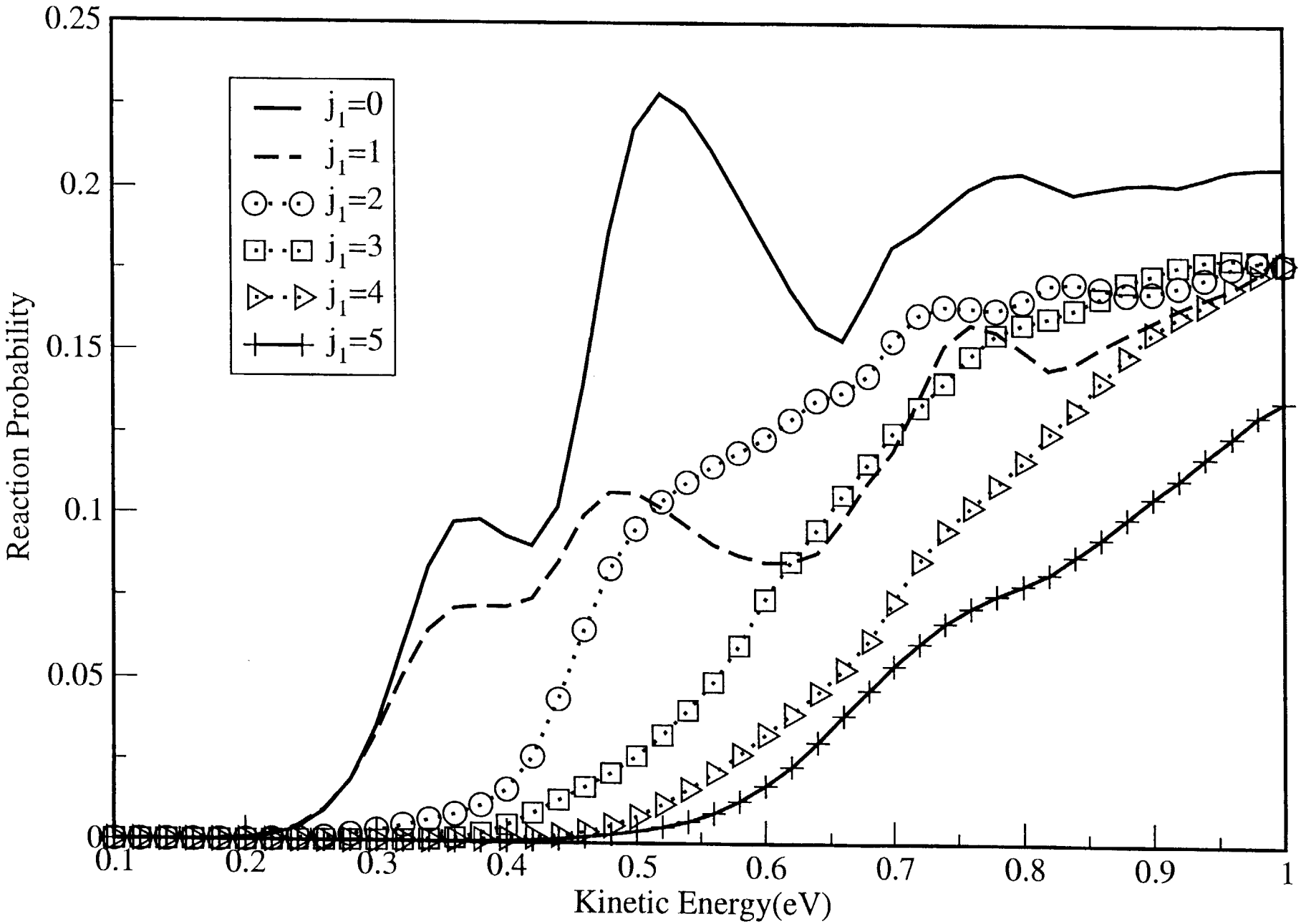
0.25
0.2
0.15
0.1
0.05
0
Reaction Probability
j1=0
j1=1
j1=2
j1=3
j1=4
j1=5
0.1
0.2
0.3
0.4
0.5
0.6
0.7
0.8
0.9
1
Kinetic Energy(eV)

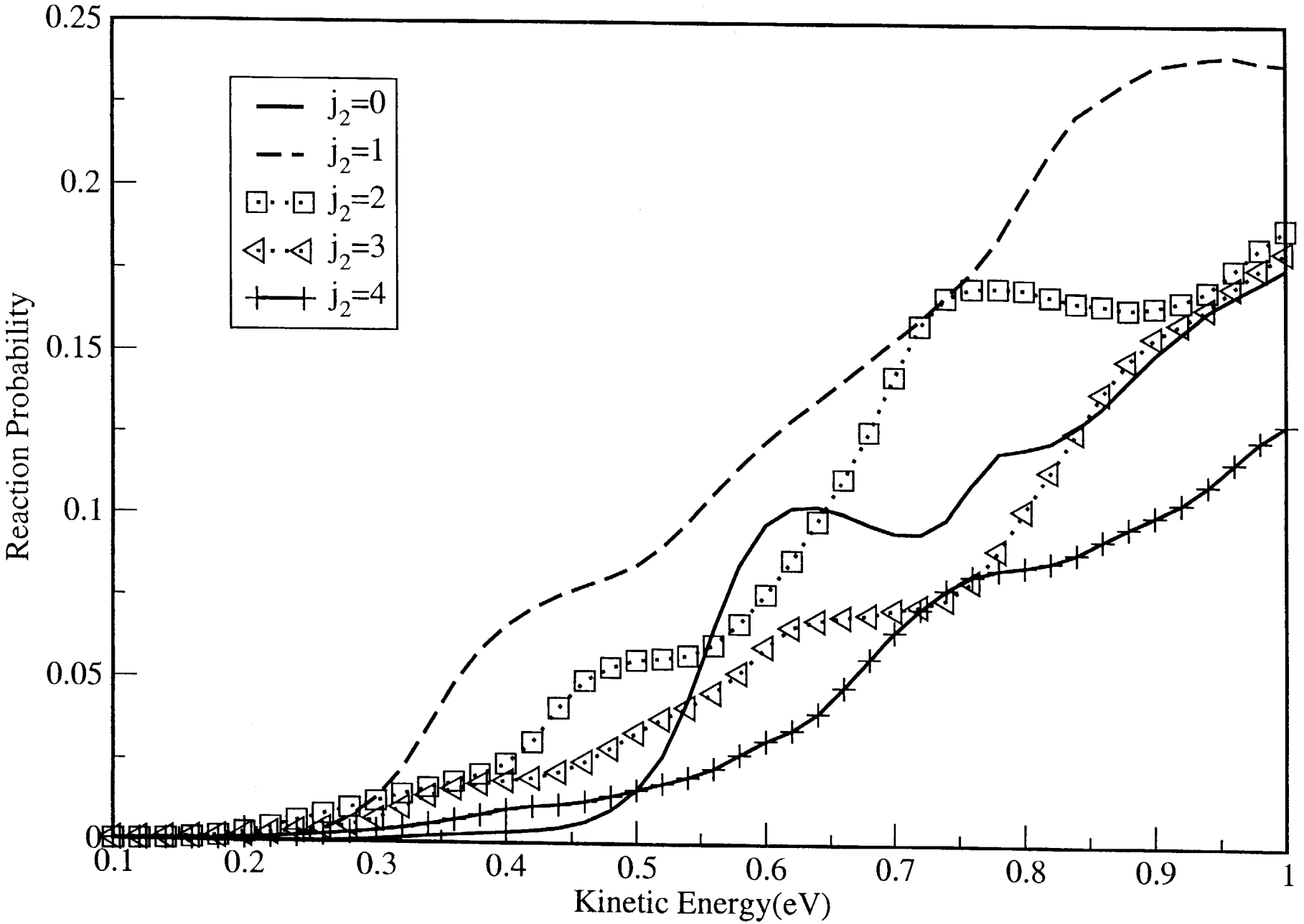
0.25
0.2
0.15
0.1
0.05
0
Reaction Probability
j_2=0
j_2=1
j_2=2
j_2=3
j_2=4
0.1
0.2
0.3
0.4
0.5
0.6
0.7
0.8
0.9
1
Kinetic Energy(eV)

Fig. 4

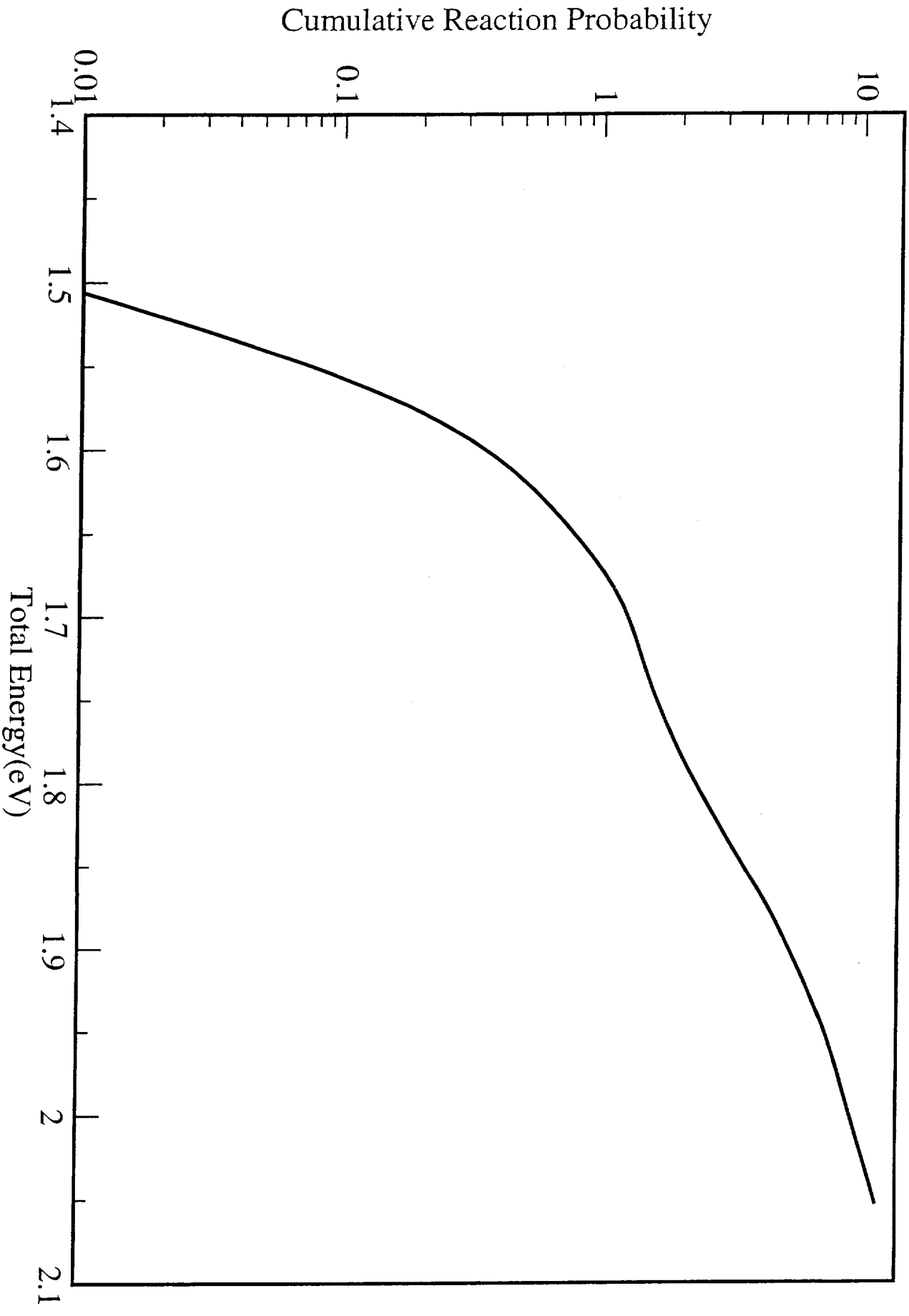
Cumulative Reaction Probability
0.01
0.1
1
10
1.4
1.5
1.6
1.7
1.8
1.9
2
2.1
Total Energy(eV)

Fig. 5

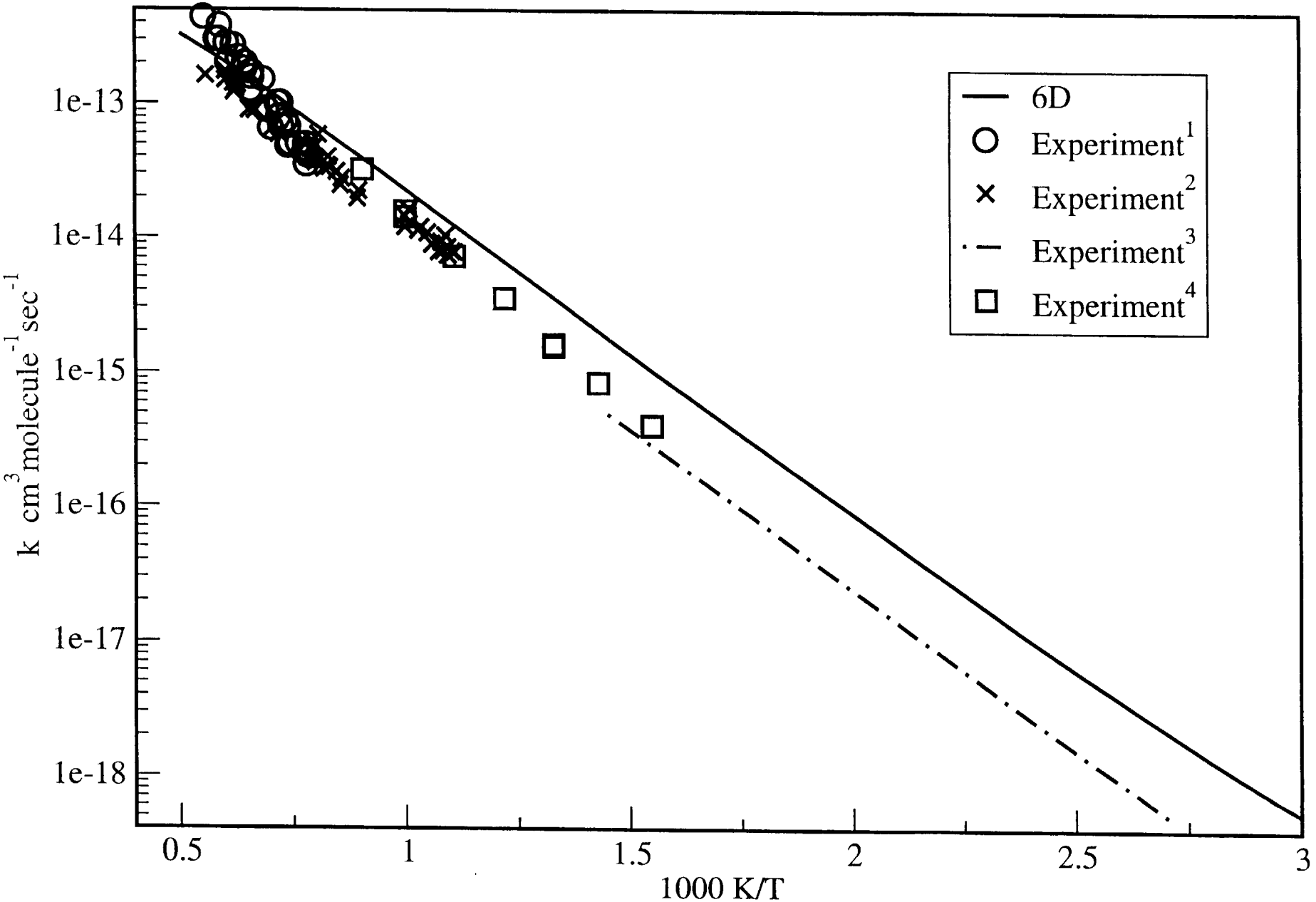
6D
Experiment[1]
Experiment[2]
Experiment[3]
Experiment[4]
1e-13
1e-14
1e-15
1e-16
1e-17
1e-18
k cm[3] molecule[-1] sec[-1]
0.5
1
1.5
2
2.5
3
1000 K/T

Fig. 6